

TRANSPARENT HELIUM IN STRIPPED ENVELOPE SUPERNOVAE

ANTHONY L. PIRO AND VIKTORIYA S. MOROZOVA

Theoretical Astrophysics, California Institute of Technology, 1200 E. California Blvd., M/C 350-17, Pasadena, CA 91125, USA; piro@caltech.edu
Received 2014 July 22; accepted 2014 August 2; published 2014 August 14

ABSTRACT

Using simple arguments based on photometric light curves and velocity evolution, we propose that some stripped envelope supernovae (SNe) show signs that a significant fraction of their helium is effectively transparent. The main pieces of evidence are the relatively low velocities with little velocity evolution, as are expected deep inside an exploding star, along with temperatures that are too low to ionize helium. This means that the helium should not contribute to the shaping of the main SN light curve, and thus the total helium mass may be difficult to measure from simple light curve modeling. Conversely, such modeling may be more useful for constraining the mass of the carbon/oxygen core of the SN progenitor. Other stripped envelope SNe show higher velocities and larger velocity gradients, which require an additional opacity source (perhaps the mixing of heavier elements or radioactive nickel) to prevent the helium from being transparent. We discuss ways in which similar analysis can provide insights into the differences and similarities between SNe Ib and Ic, which will lead to a better understanding of their respective formation mechanisms.

Key words: hydrodynamics – shock waves – supernovae: general

1. INTRODUCTION

One of the fundamental problems in stellar astrophysics is connecting supernovae (SNe) with their massive stellar progenitors. There is strong evidence that Type II-P SNe are from the core collapse of red supergiants, both via direct identification with pre-explosion imaging (Smartt et al. 2009) and modeling of their light curves (Falk & Arnett 1977; Eastman et al. 1994; Kasen & Woosley 2009; Dessart et al. 2010; Bersten et al. 2011; Dessart & Hillier 2011). In contrast, for the mass-stripped SNe (Type Ib, Ic, and IIfb), direct identification has been difficult with the exception of a few cases of yellow supergiants associated with SNe IIfb (Maund et al. 2011; Bersten et al. 2012; Van Dyk et al. 2013, 2014). Historically, there has been debate whether their mass stripping comes from the winds of effectively isolated stars or if it is due to binary interactions. However, more recently, both light curve modeling (Ensmann & Woosley 1988; Dessart et al. 2011; Benvenuto et al. 2013; Bersten et al. 2014; Fremling et al. 2014), which favors relatively low ejecta masses, and the high rates of SNe Ib and Ic (Smith et al. 2011) argue that a binary origin explains the majority of these events (also see Smith 2014).

A further complication in trying to understand the origin of mass-stripped SNe is identifying the mechanism that determines whether an SN is of Type Ib or Ic. Spectroscopically, this difference is simply attributed to a lack of observed helium, but as highlighted by Dessart et al. (2012), this does not necessarily mean that SNe Ic are intrinsically helium-poor (although see Hachinger et al. 2012). Non-thermal excitation and ionization are key for the production of He I lines (Lucy 1991). Thus an SN progenitor with helium-rich surface layers could in principle look like an SN Ib or Ic depending on the amount of mixing of ^{56}Ni . Given these complications, it would be useful to have simple rules of thumb to determine what these SNe are telling us about the presence or absence of helium and understand how it impacts other inferences about the progenitor. This is the motivation of the present work.

A further motivation is the steadily growing sample of stripped envelope SNe (Drout et al. 2011; Modjaz et al. 2014) that will continue to be discovered by current and future surveys

such as the Palomar Transient Factory (PTF; Rau et al. 2009), Pan-STARRS (Kaiser et al. 2002), the Carnegie Supernova Project (CSP; Hamuy et al. 2006), LCOGT (Brown et al. 2013), the Zwicky Transient Facility (ZTF; Law et al. 2009), ASAS-SN (Shappee et al. 2013), and LSST (LSST Science Collaboration et al. 2009). They allow events to be studied in aggregate to search for interesting trends in the ejecta masses, energetics, ^{56}Ni , and a range of other properties (Lyman et al. 2014). Such work is well suited for simple modeling to control the parameter space, but it is only useful if the limitations of such modeling are properly understood.

In Section 2, we demonstrate that the He I lines in three example SNe IIfb/Ib are a useful tracer for their photospheres. This shows that for at least the two SNe IIfb we consider, we are likely seeing deep into the SN ejecta. We make comparisons with hydrodynamic models of exploding stars to strengthen this case. Coupled with the temperature evolution and the opacity of the helium-rich surface layers presented in Section 3, we argue that a non-negligible fraction of helium is recombined in these SNe IIfb. We conclude in Section 4 with a summary of our conclusions and a discussion of future work, particularly for comparing Type Ib and Ic SNe.

2. COLOR VELOCITY EVOLUTION

As a shock passes through an exploding star, it accelerates and unbinds material. The velocity to which ejecta are accelerated can vary greatly throughout the star and is sensitive to the stellar density profile as described in Matzner & McKee (1999). Roughly speaking, the velocity decreases as the shock moves out and sweeps up more mass, but it can also accelerate when the density decreases rapidly, especially at the star's surface. Therefore, high velocities and large velocity gradients indicate that observations are probing material with a large density gradient, likely near the surface of the star.

These features can be seen in the upper panel of Figure 1, which shows the terminal velocity profile for a range of different explosion energies in a star that has a mass of $\sim 5 M_{\odot}$ at core collapse. This star was generated from a $15 M_{\odot}$ zero-age main-sequence star using the one-dimensional (1D) stellar evolution

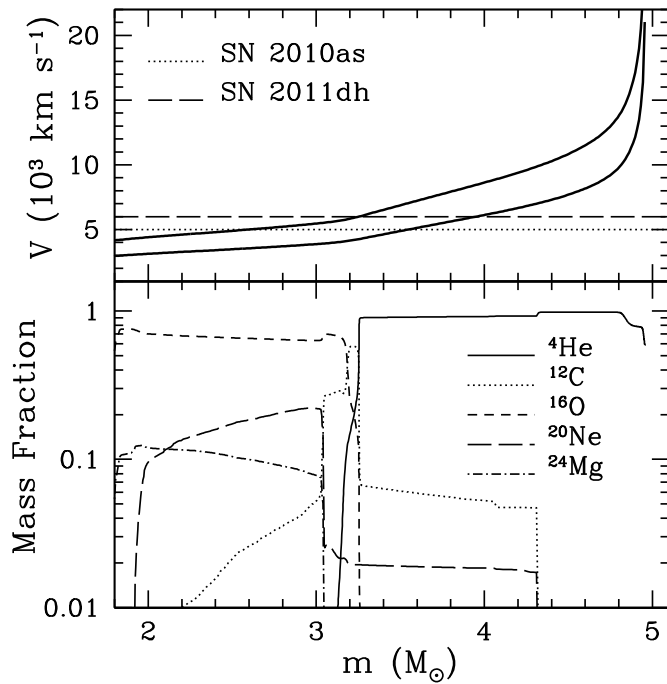


Figure 1. Profile of an exploding star as a function of mass coordinate. The model is a $15 M_{\odot}$ zero-age main-sequence star with its hydrogen envelope removed to simulate binary mass loss. The upper panel shows terminal velocity profiles of 10^{51} and 2×10^{51} erg explosions (solid lines, bottom and top, respectively). The horizontal lines show typical He I velocities for SNe 2010as and 2011dh to help guide the eye. The bottom panel shows the composition of the most abundant elements at the moment of core collapse.

code MESA (Paxton et al. 2013). Using the overshooting and mixing parameters recommended by Sukhbold & Woosley (2014), the star is evolved until a large entropy jump between the core and envelope was established. The convective envelope is removed to mimic mass loss during a common envelope phase and then the star continues to evolve up to core collapse. A shock is initiated by heating the star at a mass coordinate of $m = 1.5 M_{\odot}$, and the subsequent hydrodynamic evolution is followed using our 1D Lagrangian SN explosion code (SNEC; V. S. Morozova et al. in preparation, which follows the numerical hydrodynamic scheme of Mezzacappa & Bruenn 1993). The main features to note are the great acceleration of the shock near the surface and the more modest acceleration at the boundary between the carbon/oxygen layers and the helium-rich surface layers. In the bottom panel of Figure 1, we plot the composition of some of the most abundant elements in the star prior to explosion.

Recently, Folatelli et al. (2014) pointed out that some stripped envelope SNe appear to have anomalously low He I velocities in the range of $4000\text{--}8000 \text{ km s}^{-1}$ with one of the prime examples being SN 2010as (see Figure 2). This is lower than the typical velocities of $10,000\text{--}15,000 \text{ km s}^{-1}$ (see the surface layers in Figure 1) typically associated with the photosphere. In addition, the evolution with time is much flatter, which is again not expected given the high velocity gradient in the surface layers.

To better understand what is implied by these seemingly low velocities, it is helpful to consider the velocity of material at the color depth (also known as the thermalization depth), henceforth referred to as the color velocity V_c . For a blackbody with temperature T_{BB} and color radius r_c , the bolometric luminosity is $L = 4\pi r_c^2 \sigma_{\text{SB}} T_{\text{BB}}^4 / \tau_c$, where σ_{SB} is the Stefan–Boltzmann constant and τ_c is the optical depth at the color depth. Substituting

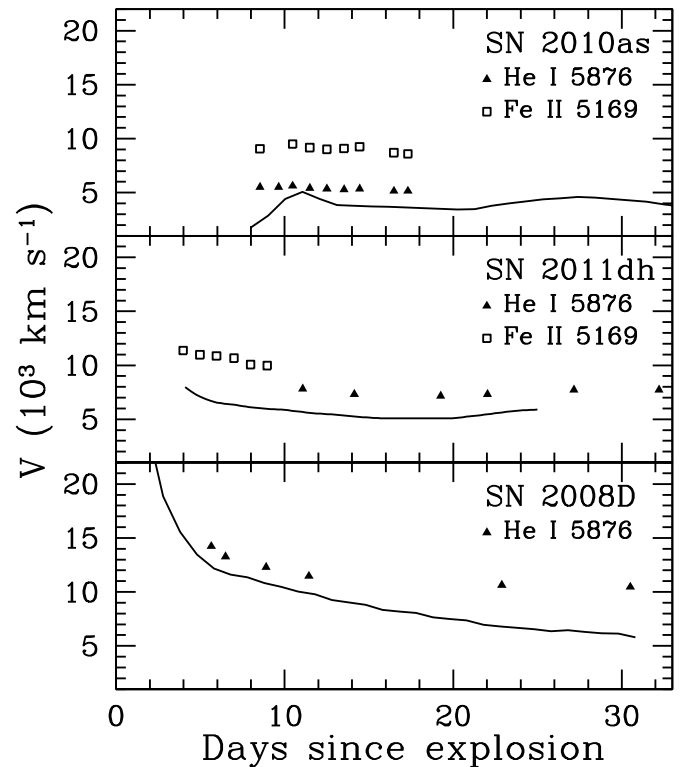


Figure 2. In each case the solid line marks V_c in the SN that was found using Equation (1) with $\tau_c = 1$. The upper two panels are Type IIb SNe that have been noted for their especially low velocity helium, while the bottom panel is a SN Ib with a more typical velocity evolution. Nevertheless, in all three cases, V_c is similar but below the helium velocity.

$$r_c = V_c t,$$

$$V_c = \frac{1}{t} \left(\frac{L \tau_c}{4\pi \sigma_{\text{SB}} T_{\text{BB}}^4} \right)^{1/2}. \quad (1)$$

The color radius r_c is roughly where an incoming photon would experience at least one absorption rather than just a scattering and thus where the observed blackbody temperature is determined (see Nakar & Sari 2010; Piro & Nakar 2013). The color radius is in general slightly deeper than the actual photosphere. Nevertheless, V_c should provide a useful diagnostic for roughly tracking the photospheric velocity.

Equation (1) with $\tau_c = 1$ is used to analyze three different events: the Type IIb SNe 2010as (Folatelli et al. 2014) and 2011dh (Marion et al. 2014) and the Type Ib SN 2008D (Modjaz et al. 2009). Setting $\tau_c = 1$ gives a lower limit on V_c , since $\tau_c > 1$. Although SNe IIb have a thin hydrogen layer at the surface (Woosley et al. 1994; Bersten et al. 2012; Nakar & Piro 2014), this is sufficiently low mass that it will be optically thin at the times we consider and not affect our arguments. In Figure 2, we also plot the measured He I 5876 absorption line velocities and, in two cases, the Fe II 5169 velocities. In all three SNe, V_c is similar to but less than the He I velocity. This fact argues that the helium is indeed tracking the photosphere, and that τ_c cannot be too far from unity. We conclude that even when the velocity is low there is nothing intrinsically anomalous about the He I velocities. Rather they are simply consistent with the velocity of the ejecta as inferred from the luminosity and temperature.

As a comparison, in the upper panel of Figure 1 we plot horizontal lines roughly at the He I velocities for SNe 2010as and 2011dh. In both cases, these velocities are similar to what

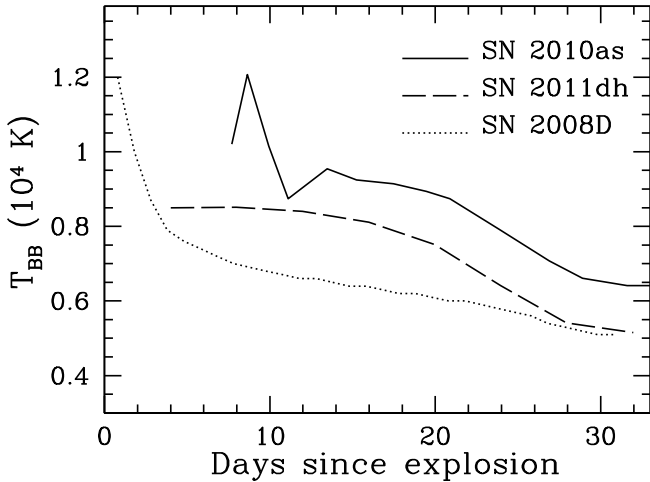


Figure 3. Blackbody temperature as a function of time for each of the three SNe using the data from Folatelli et al. (2014), Marion et al. (2014), and Modjaz et al. (2009).

is expected near the boundary between the carbon/oxygen inner layers and the helium-rich surface layers. Furthermore, one can see that the velocity profile near these regions is much shallower than the surface velocity, again consistent with the observed He I features. Although this comparison cannot provide a quantitative result, at least qualitatively it appears that for SNe 2010as and 2011dh we are looking deep into the ejecta. In contrast, SN 2008D shows higher velocities with a larger velocity gradient consistent with the outer portions of the star, and thus we are not looking as deep into the ejecta.

3. TEMPERATURE AND OPACITY

To understand why the He I and V_c have relatively small velocities, it is helpful to consider the actual blackbody temperatures that are being observed. In Figure 3, we plot the temperature evolution for each of the three SNe. In comparison, in Figure 4, we plot the opacity as a function of temperature for helium-rich material (Badnell et al. 2005 and references therein), as is expected in the outer layers of these stripped envelope progenitors. Above a temperature of $\approx 1.2 \times 10^4$ K, the opacity is $\approx 0.1 \text{ cm}^2 \text{ g}^{-1}$, consistent with electron scattering from material with one electron per four nucleons (i.e., singly ionized helium). Below this temperature, the opacity is almost zero and the material is effectively transparent. We also consider a mixture with 10% carbon and oxygen. This particular plot uses a density of $10^{-11} \text{ g cm}^{-3}$, but the threshold at which this happens is not strongly dependent on density. Only once the material is largely carbon/oxygen does the opacity increase much for low T .

Combining Figures 3 and 4 with the low and flat He I velocities, we conclude that a large fraction of helium in SNe 2010as and 2011dh is transparent. To be clear, it is true that helium absorption lines are seen in all of these SNe, but this is only at a few specific wavelengths. What we are arguing is that across the majority of the spectrum, the helium-rich material is not drastically impacting the time it takes photons to diffuse out of the expanding ejecta. One potential complication is if there are opacity sources that increase the opacity that are not taken into account in Figure 4. A standard practice for light curve modeling codes is to invoke an opacity floor (Bersten et al. 2011, and references therein). This replicates physics such as bound-free and bound-bound absorptions, and non-thermal excitation or ionization of electrons by Compton

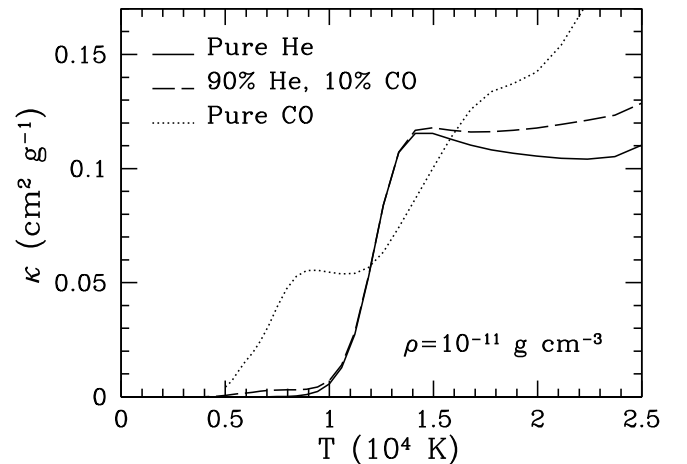


Figure 4. Rosseland mean opacity as a function of temperature and at a representative density of $10^{-11} \text{ g cm}^{-3}$ (κ is weakly dependent on density). We plot a composition of pure helium (solid line), helium with a 10% mass fraction carbon/oxygen (dashed line), and pure carbon/oxygen (dotted line).

scattering of γ -rays (although Kleiser & Kasen 2014 show that at least the bound-bound opacity for pure helium is negligible). Nevertheless, the close match between the He I line velocities and V_c in Figure 2 argues that this opacity floor cannot be too large and that a non-negligible fraction of the helium is recombined and not providing a large opacity. Although SN 2008D has even colder temperatures, it does not have the same low velocities or flat velocity evolution. This SN therefore requires an additional opacity source within its helium-rich surface layers, such as the mixing of metals or ^{56}Ni , the latter of which could assist in helium ionization. Calculations using an opacity floor should therefore be more appropriate for events with velocities like SN 2008D.

The inference of transparent material has implications for studies that use simple models to constrain the properties of the SNe from their photometric light curves. The basic idea of these works is to relate the rise time of the SN to the ejecta mass, $t_{\text{rise}} \propto (\kappa M_{\text{ej}}/v_{\text{ej}}c)^{1/2}$, where M_{ej} and v_{ej} are the typical mass and velocity of the ejecta, respectively (Arnett 1982). This should work as long as the opacity κ is representative of the majority of the material, but not if κ varies by a large amount which happens if some material is transparent. Recently Lyman et al. (2014) used similar semi-analytic methods to study the ejecta masses in 38 Type IIb, Ib, Ic, and Ic-BL SNe. One particularly striking conclusion was that the majority of these stripped-envelope SNe have rather similar ejecta masses in the range of $\sim 1-5 M_{\odot}$. If the typical understanding of the difference between SNe Ib and Ic is true, namely that SNe Ic have additional mass loss to remain their helium envelopes, one would instead expect, on average, larger ejecta masses from SNe Ib than from SNe Ic. Our discussion here demonstrates that indeed the SNe Ib could have more ejecta overall, but the mass of the helium does not impact the light curve width because it is transparent. What these measurements are able to constrain with certainty is the mass of the progenitor's carbon/oxygen core. In the future, consideration of the velocity evolution of each SN should be taken into account when assessing each inferred ejecta mass.

4. CONCLUSION AND DISCUSSION

We have inferred the time-dependent color velocity V_c for three different SNe and compared it with hydrodynamic

models of mass-stripped star explosions. We then argued that the combination of (1) blackbody temperatures too low for helium ionization, (2) relatively low He I velocities with a flat evolution in time, and (3) a V_c evolution that indicates the He I velocities are representative of the photosphere suggest that a non-negligible amount of helium is effectively transparent in SNe 2010as and 2011dh. This could result in a solar mass or more being missed by simple models attempting to infer the ejecta mass. *Even in detailed numerical studies of these events, constraining the total ejecta mass may be difficult.* This is because even if a given model is shown to fit, a similarly good fit may be possible with an additional amount of helium (which may require corresponding adjustments to the explosion energy). Future numerical modeling needs to quantify just how much helium can actually be hidden.

In contrast, SN 2008D has higher velocities and a larger velocity gradient, consistent with material near the surface of a star, even though its T_{BB} is lower than that of the other two SNe. This indicates an additional opacity source is required to prevent the helium from being more transparent. We hope that our results will motivate similar analyses of V_c in future SN studies. This was recently done for the SN Ib iPTF13bvn (Fremming et al. 2014) and again $T_{\text{BB}} < 10^4$ K and V_c is similar to the He I. This work constrained the ejecta mass to be $\approx 2 M_{\odot}$ (also see Bersten et al. 2014), and thus would rule out a Wolf–Rayet progenitor (as suggested by pre-explosion photometry; Cao et al. 2013). Although transparent helium may not be enough to reconcile this ejecta mass difference with a Wolf–Rayet star, it could easily be a significant correction.

To maximize the usefulness of such studies, it will be important to have measurements of L , T_{BB} , and t , so that Equation (1) can be applied. This puts emphasis on covering all wavelengths so that the bolometric luminosity and blackbody temperature can be accurately inferred (see the discussion in Marion et al. 2014). Infrared can be helpful for correctly measuring the He I velocities since at optical wavelengths He I absorption features can potentially be confused with other elements (although, in any case, the lowest securely observed He I velocity should be used to get as close to the photosphere as possible). Getting an accurate t requires that the SN be detected as early as possible since in cases where a first peak in the light curve is not seen it can be difficult to know exactly when the explosion happened (Piro & Nakar 2013).

Comparing and contrasting this type of analysis between SNe Ib and Ic may be especially instructive for understanding their respective origins. The SN shock will always accelerate material to high velocities near the surface of the star as shown in Figure 1. *If SNe Ic are truly devoid of helium, then these large velocities will occur in higher opacity carbon/oxygen material rather than lower opacity helium material.* This should give rise to $V_c \approx 10,000\text{--}15,000$ km s $^{-1}$ with a larger velocity gradient as is seen for SN 2008D. If SNe Ic always show such a V_c evolution that is consistent with no helium present, this would be strong evidence that SNe Ic experience more mass stripping than SNe Ib. If instead there is evidence for transparent helium in some SNe Ic (i.e., they show V_c evolution similar to SNe 2010as and 2011dh), this would argue that there is transparent helium material present. In this case, the relative deposition of helium versus ^{56}Ni may be an important factor for deciding the classification, as described by Dessart et al. (2012), so that

issues like mixing, turbulence, rotation, and asymmetries need to be more fully considered for generating a Type Ib or Ic. No matter the solution, determining between these scenarios would be an important step forward for our understanding of stripped-envelope SNe.

We thank Drew Clausen for generating the $15 M_{\odot}$ model used for Figure 1; Melina Bersten and Mattias Ergon for helpful discussions; and Dan Kasen, Ehud Nakar, Christian Ott, and Nathan Smith for feedback on previous drafts. We also thank the Carnegie Supernova Project, and in particular Mark Phillips, for generously hosting ALP at the CSP II Team Meeting at St. George Island, FL where this work was inspired. This work was supported through NSF grants AST-1205732, PHY-1068881, PHY-1151197, PHY-1404569, and the Sherman Fairchild Foundation.

REFERENCES

- Arnett, W. D. 1982, *ApJ*, 253, 785
- Badnell, N. R., Bautista, M. A., Butler, K., et al. 2005, *MNRAS*, 360, 458
- Benvenuto, O. G., Bersten, M. C., & Nomoto, K. 2013, *ApJ*, 762, 74
- Bersten, M. C., Benvenuto, O., & Hamuy, M. 2011, *ApJ*, 729, 61
- Bersten, M. C., Benvenuto, O. G., Folatelli, G., et al. 2014, arXiv:1403.7288
- Bersten, M. C., Benvenuto, O. G., Nomoto, K., et al. 2012, *ApJ*, 757, 31
- Brown, T. M., Baliber, N., Bianco, F. B., et al. 2013, *PASP*, 125, 1031
- Cao, Y., Kasliwal, M. M., Arcavi, I., et al. 2013, *ApJL*, 775, L7
- Dessart, L., & Hillier, D. J. 2011, *MNRAS*, 410, 1739
- Dessart, L., Hillier, D. J., Li, C., & Woosley, S. 2012, *MNRAS*, 424, 2139
- Dessart, L., Hillier, D. J., Livne, E., et al. 2011, *MNRAS*, 414, 2985
- Dessart, L., Livne, E., & Waldman, R. 2010, *MNRAS*, 408, 827
- Drout, M. R., Soderberg, A. M., Gal-Yam, A., et al. 2011, *ApJ*, 741, 97
- Eastman, R. G., Woosley, S. E., Weaver, T. A., & Pinto, P. A. 1994, *ApJ*, 430, 300
- Ensmann, L. M., & Woosley, S. E. 1988, *ApJ*, 333, 754
- Falk, S. W., & Arnett, W. D. 1977, *ApJS*, 33, 515
- Folatelli, G., Bersten, M. C., Kuncarayakti, H., et al. 2014, arXiv:1407.6711
- Fremming, C., Sollerman, J., Taddia, F., et al. 2014, *A&A*, 565, A114
- Hachinger, S., Mazzali, P. A., Taubenberger, S., et al. 2012, *MNRAS*, 422, 70
- Hamuy, M., Folatelli, G., Morrell, N. I., et al. 2006, *PASP*, 118, 2
- Kaiser, N., Aussen, H., Burke, B. E., et al. 2002, *Proc. SPIE*, 4836, 154
- Kasen, D., & Woosley, S. E. 2009, *ApJ*, 703, 2205
- Kleiser, I. K. W., & Kasen, D. 2014, *MNRAS*, 438, 318
- Law, N. M., Kulkarni, S. R., Dekany, R. G., et al. 2009, *PASP*, 121, 1395
- LSST Science Collaboration, Abell, P. A., Allison, J., et al. 2009, arXiv:0912.0201
- Lucy, L. B. 1991, *ApJ*, 383, 308
- Lyman, J., Bersier, D., James, P., et al. 2014, arXiv:1406.3667
- Marion, G. H., Vinko, J., Kirshner, R. P., et al. 2014, *ApJ*, 781, 69
- Matzner, C. D., & McKee, C. F. 1999, *ApJ*, 510, 379
- Maund, J. R., Fraser, M., Ergon, M., et al. 2011, *ApJL*, 739, L37
- Mezzacappa, A., & Bruenn, S. W. 1993, *ApJ*, 405, 669
- Modjaz, M., Blondin, S., Kirshner, R. P., et al. 2014, *AJ*, 147, 99
- Modjaz, M., Li, W., Butler, N., et al. 2009, *ApJ*, 702, 226
- Nakar, E., & Piro, A. L. 2014, *ApJ*, 788, 193
- Nakar, E., & Sari, R. 2010, *ApJ*, 725, 904
- Paxton, B., Cantiello, M., Arras, P., et al. 2013, *ApJS*, 208, 4
- Piro, A. L., & Nakar, E. 2013, *ApJ*, 769, 67
- Rau, A., Kulkarni, S. R., Law, N. M., et al. 2009, *PASP*, 121, 1334
- Shappee, B. J., Prieto, J. L., Grupe, D., et al. 2013, *ApJ*, 788, 48
- Smartt, S. J., Eldridge, J. J., Crockett, R. M., & Maund, J. R. 2009, *MNRAS*, 395, 1409
- Smith, N. 2014, arXiv:1402.1237
- Smith, N., Li, W., Filippenko, A. V., & Chornock, R. 2011, *MNRAS*, 412, 1522
- Sukhbold, T., & Woosley, S. E. 2014, *ApJ*, 783, 10
- Van Dyk, S. D., Zheng, W., Clubb, K. I., et al. 2013, *ApJL*, 772, L32
- Van Dyk, S. D., Zheng, W., Fox, O. D., et al. 2014, *AJ*, 147, 37
- Woosley, S. E., Eastman, R. G., Weaver, T. A., & Pinto, P. A. 1994, *ApJ*, 429, 300